On the Solid Solutions $Eu_{1-x}Pt_2In_x$, $Gd_{1-x}Pt_2In_x$, and $Tm_{1-x}Ni_2In_x$

Mar'yana Lukachuk[a], Yaroslav M. Kalychak[b], Tom Nilges[a], and Rainer Pöttgen[a]

[a] Institut für Anorganische und Analytische Chemie and NRW Graduate School of Chemistry, Westfälische Wilhelms-Universität Münster, Corrensstraße 36, 48149 Münster, Germany
[b] Inorganic Chemistry Department, Ivan Franko National University of Lviv, Kyryla and Mephodiya Street 6, 79005 Lviv, Ukraine

Reprint requests to R. Pöttgen. E-mail: pottgen@uni-muenster.de

Z. Naturforsch. **60b,** 393 – 397 (2005); received January 14, 2005

The binary cubic Laves phases $EuPt_2$, $GdPt_2$, and $TmNi_2$ form extended solid solutions $Eu_{1-x}Pt_2In_x$, $Gd_{1-x}Pt_2In_x$, and $Tm_{1-x}Ni_2In_x$. Samples within these homogeneity ranges have been prepared from the elements by arc-melting on water-cooled copper chills or by induction melting in sealed tantalum tubes and subsequent annealing. The indides were characterized by X-ray powder and single crystal diffraction: $MgCu_2$ type, $Fd\bar{3}m$, $a = 770.68(6)$ pm, $wR2 = 0.0251$, 67 F^2 values, 6 variables for $Eu_{0.94(3)}Pt_2In_{0.06(3)}$, $a = 769.16(6)$ pm, $wR2 = 0.0244$, 67 F^2 values, 6 variables for $Eu_{0.85(2)}Pt_2In_{0.15(2)}$, $a = 760.12(9)$ pm, $wR2 = 0.0693$, 65 F^2 values, 6 variables for $Gd_{0.79(5)}Pt_2In_{0.21(5)}$, and $MgCu_4Sn$ type, $F\bar{4}3m$, $a = 700.27(6)$ pm, $wR2 = 0.0368$, BASF = 0.13(2), 175 F^2 values, 8 variables for $TmNi_4In$. The platinum and nickel atoms build up three-dimensional networks of corner-sharing $Pt_{4/2}$ and $Ni_{4/2}$ tetrahedra. These networks leave larger voids of coordination number 16 that are filled with the rare earth (*RE*) and the indium atoms. While the thulium and indium atoms are ordered in $TmNi_4In$, one observes mixed *RE*/In occupancies in $Eu_{0.94(3)}Pt_2In_{0.06(3)}$, $Eu_{0.85(2)}Pt_2In_{0.15(2)}$, and $Gd_{0.79(5)}Pt_2In_{0.21(5)}$.

Key words: Solid Solution, Crystal Structure, Solid State Synthesis

Introduction

Among the binary intermetallic compounds, the Laves phases AB_2 [1] play an important role. So far more than 1600 intermetallics crystallize with the structure types $MgCu_2$, $MgNi_2$, and $MgZn_2$ [2]. Especially those Laves phases with a rare earth or actinoid metal on the *A* site have attracted considerable interest because of their interesting magnetic and electrical properties. As an example we present the $EuPt_2$ structure [3] in Fig. 1. The platinum atoms build up a three-dimensional network of corner-sharing tetrahedra. The larger voids of this network are filled by the europium atoms. The latter have coordination number 16 in the form of a Friauf polyhedron.

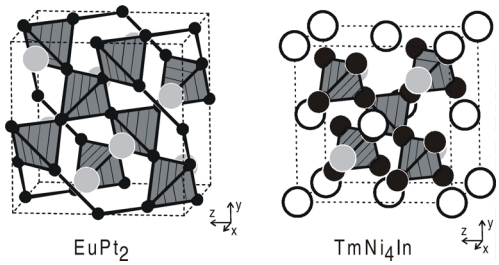

Fig. 1. The crystal structures of $EuPt_2$ ($MgCu_2$ type, space group $Fd\bar{3}m$) and $TmNi_4In$ ($MgCu_4Sn$ type, space group $F\bar{4}3m$). The rare earth metal, transition metal, and indium atoms are drawn as medium gray, filled, and open circles, respectively. The three-dimensional networks of corner-sharing $Pt_{4/2}$ and $Ni_{4/2}$ tetrahedra are emphasized.

This magnetic substructure can be *diluted*, since it is possible to substitute every other rare earth atom in an ordered manner. This is actually the $MgCu_4Sn \equiv (Mg_{0.5}Sn_{0.5})Cu_2$ structure [4, 5]. The ordering results in a symmetry reduction *via* a *translationengleiche* transition of index 2 (t2) from $Fd\bar{3}m$ to $F\bar{4}3m$. This *translationengleiche* symmetry reduction only changes the subcell intensities and twinning by inversion might occur. Thus, only precise single crystal X-ray data reveal the degree of ordering.

Several Laves phases with platinum as *B* element component have large homogeneity ranges. The change in composition has a distinct influence on the physical properties [3, 6 – 9, and ref. therein]. Other Laves phases like $TmNi_2$ [10 – 13] form complex superstructures. Several $MgCu_4Sn$ type compounds have

Table 1. Lattice parameters of cubic $MgCu_2$ and $MgCu_4Sn$ type indides.

Composition	a (pm)	V (nm^3)	Reference
$EuPt_2$	771.4	0.4590	[3]
0.75Eu:2Pt:0.25In[a]	771.34(9)	0.4589	this work
$Eu_{0.94(3)}Pt_2In_{0.06(3)}$[b]	770.68(6)	0.4577	this work
$Eu_{0.85(2)}Pt_2In_{0.15(2)}$[b]	769.16(6)	0.4550	this work
$EuPt_4In$	766.6	0.4505	[15]
$GdPt_2$	763.5	0.4451	[8]
0.75Gd:2Pt:0.25In[a]	759.6(1)	0.4383	this work
$Gd_{0.79(5)}Pt_2In_{0.21(5)}$[b]	760.12(9)	0.4392	this work
$GdPt_4In$	756.4	0.4328	[15]
$TmNi_2$	696.5–709.5	0.3379–0.3572	[10]
$TmNi_2$	710.86	0.3592	[11]
$TmNi_2$	710.5	0.3587	[12]
$TmNi_2$[a]	711.40(9)	0.3600	this work
$Tm_{0.90}Ni_2In_{0.10}$[a]	709.1(1)	0.3566	this work
$Tm_{0.74}Ni_2In_{0.26}$[a]	705.5(1)	0.3511	this work
$Tm_{0.60}Ni_2In_{0.40}$[a]	700.0(1)	0.3430	this work
$TmNi_4In$[a]	699.4(1)	0.3421	this work
$TmNi_4In$[b]	700.27(6)	0.3434	this work
$TmNi_4In$	699.3	0.3420	[14]

[a] Lattice parameters from Guinier powder data. The compositions listed here correspond to the starting compositions of the sample preparation; [b] lattice parameters from diffractometer measurements. These compositions have been refined from the single crystal data.

been investigated on the basis of X-ray powder data [2], but more detailed studies on solid solutions, where the *A* site is partly replaced by a main group element are rare. In that context we were interested in the Laves phases $TmNi_2$, $EuPt_2$, and $GdPt_2$ with respect to their solid solutions $Tm_{1-x}Ni_2In_x$, $Eu_{1-x}Pt_2In_x$, and $Gd_{1-x}Pt_2In_x$. So far only X-ray powder data of $TmNi_4In$ [14], $EuPt_4In$, and $GdPt_4In$ [15] have been reported. Herein we present single crystal data of compounds within these solid solutions.

Experimental Section

Synthesis

Starting materials for the preparation of the various samples with stoichiometries within the solid solution ranges $Tm_{1-x}Ni_2In_x$, $Eu_{1-x}Pt_2In_x$, and $Gd_{1-x}Pt_2In_x$ were ingots of thulium, europium, and gadolinium (Chempur or Johnson Matthey), nickel wire (∅0.38 mm) or nickel powder (Johnson Matthey), platinum powder (*ca*. 200 mesh, Degussa-Hüls), and indium tear drops (Johnson Matthey), all with stated purities $> 99.9\%$. The elements were weighed in the atomic ratios listed in Table 1. The gadolinium and thulium based samples were arc-melted [16] under an argon pressure of *ca*. 600 mbar. The argon was purified over titanium sponge (900 K), silica gel, and molecular sieves. The product buttons were re-melted three times in order to ensure homogeneity. The total weight losses after the arc-melting procedures were always smaller than 0.5 weight-%. The gadolinium sample was not well crystallized. In order to get better crystals for X-ray investigations the sample was placed in a sealed tantalum tube, which was subsequently enclosed in an evacuated silica ampoule. In a box furnace the sample was first heated for 4 h at 1270 K, followed by slow cooling to 770 K at a rate of 3 K/h. Finally the sample was rapidly cooled to room temperature. The $Tm_{1-x}Ni_2In_x$ samples were homogenized by annealing in evacuated quartz ampoules at 870 K during one month in a box furnace. After the annealing procedure the samples were quenched in cold water.

The europium based samples were prepared by high-frequency melting [17] of the elements in a sealed tantalum ampoule. This prevents europium loss which would occur during an arc-melting procedure because of the low boiling temperature of europium (1870 K). The sample was first heated up to about 1300 K and then slowly cooled to room temperature within two hours. The sample could easily be separated from the tantalum tube after the melting procedure.

All samples were obtained in amounts of about 1 g. Compact pieces are light grey with metallic luster. The samples are stable in moist air. No decomposition was observed after several weeks.

X-ray data and structure refinement

The annealed samples were characterized through Guinier powder patterns. The Guinier camera was operated with Cu-$K_{\alpha 1}$ radiation and an image plate system (Fujifilm–BAS1800). α-Quartz ($a = 491.30$, $c = 540.46$ pm) was used as an internal standard. The cubic lattice parameters (Table 1) were obtained from least-squares fits of the Guinier data. The correct indexing was ensured through intensity calculations [18], using the atomic parameters obtained from the structure refinements. Some samples were additionally investigated on a Stoe Stadi P powder diffractometer with Cu-$K_{\alpha 1}$ radiation and silicon ($a = 543.07$ pm) as an external standard.

Small irregularly shaped crystals were selected from the different samples. They were glued to quartz fibres using bees wax and first examined on a Buerger precession camera (equipped with an image plate and white Mo radiation) in order to establish the suitability for intensity data collection. Single crystal intensity data of $Eu_{0.94(3)}Pt_2In_{0.06(3)}$, $Eu_{0.85(2)}Pt_2In_{0.15(2)}$, and $TmNi_4In$ were collected at room temperature by use of a four-circle diffractometer (CAD4) with graphite monochromatized Mo-K_α radiation and a scintillation counter with pulse-height discrimination. The scans were taken in the $\omega/2\theta$ mode and empirical absorption corrections were applied on the basis of Ψ-scan data. The $Gd_{0.79(5)}Pt_2In_{0.21(5)}$ data set was collected on a STOE IPDS-II diffractometer with monochromated Mo-K_α radiation in oscillation mode. The absorption correction was numerical.

Table 2. Crystal data and structure refinement for $Eu_{0.94(3)}Pt_2In_{0.06(3)}$, $Eu_{0.85(2)}Pt_2In_{0.15(2)}$, $Gd_{0.79(5)}Pt_2In_{0.21(5)}$, and $TmNi_4In$.

Empirical formula	$Eu_{0.94(3)}Pt_2In_{0.06(3)}$	$Eu_{0.85(2)}Pt_2In_{0.15(2)}$	$Gd_{0.79(5)}Pt_2In_{0.21(5)}$	$TmNi_4In$
Molar mass [g/mol]	539.96	536.39	538.47	518.59
Structure type	$MgCu_2$	$MgCu_2$	$MgCu_2$	$MgCu_4Sn$
Space group, Z	$Fd\bar{3}m$, 8	$Fd\bar{3}m$, 8	$Fd\bar{3}m$, 8	$F\bar{4}3m$, 4
Unit cell dimensions	Table 1	Table 1	Table 1	Table 1
Calculated density [g/cm^3]	15.67	15.66	16.29	10.07
Crystal size [μm^3]	$10\times10\times40$	$10\times40\times50$	$20\times30\times70$	$10\times20\times50$
Detector distance [mm]	–	–	60	–
Exposure time [min]	–	–	18	–
ω Range; increment [°]	–	–	0 – 180; 1.0	–
Integr. param. A, B, EMS	–	–	15.5; 4.5; 0.020	–
Transm. ratio [max/min]	2.17	3.79	5.68	1.90
Absorption coefficient [mm^{-1}]	147.6	146.8	152.4	53.6
F(000)	1745	1735	1735	920
θ Range [°]	4 to 35	4 to 35	4 to 35	5 to 45
Range in h	$-12 \le h \le 0$	±12	±12	±13
Range in k	$-12 \le k \le 0$	±12	±12	±13
Range in l	±12	±12	±12	±13
Total no. reflections	501	1826	1491	2740
Independent reflections	67	67	65	175
	($R_{int} = 0.0673$)	($R_{int} = 0.0863$)	($R_{int} = 0.1538$)	($R_{int} = 0.0461$)
Reflections with $I > 2\sigma(I)$	60	64	65	167
	($R_\sigma = 0.0332$)	($R_\sigma = 0.0205$)	($R_\sigma = 0.0583$)	($R_\sigma = 0.0138$)
Data / parameters	67 / 6	67 / 6	65 / 6	175 / 8
Goodness-of-fit on F^2	0.995	1.215	1.461	1.218
Final R indices [$I > 2\sigma(I)$]	$R1 = 0.0161$	$R1 = 0.0106$	$R1 = 0.0247$	$R1 = 0.0171$
	$wR2 = 0.0247$	$wR2 = 0.0240$	$wR2 = 0.0247$	$wR2 = 0.0363$
R Indices (all data)	$R1 = 0.0208$	$R1 = 0.0117$	$R1 = 0.0693$	$R1 = 0.0185$
	$wR2 = 0.0251$	$wR2 = 0.0244$	$wR2 = 0.0693$	$wR2 = 0.0368$
BASF	–	–	–	0.13(2)
Extinction coefficient	0.00053(5)	0.00104(7)	0.0015(3)	0.0037(3)
Largest diff. peak and hole	1.94 / –1.94 e/Å^3	1.59 / –0.98 e/Å^3	2.62 / –2.54 e/Å^3	2.60 / –1.82 e/Å^3

Table 3. Atomic coordinates and isotropic displacement parameters (pm^2) for $Eu_{0.94(3)}Pt_2In_{0.06(3)}$, $Eu_{0.85(2)}Pt_2In_{0.15(2)}$, $Gd_{0.79(5)}Pt_2In_{0.21(5)}$, and $TmNi_4In$. U_{eq} is defined as one third of the trace of the orthogonalized U_{ij} tensor.

Atom	Wyckoff position	Occupancy	x	y	z	U_{eq}
$Eu_{0.94(3)}Pt_2In_{0.06(3)}$ ($Fd\bar{3}m$)						
Eu/In	8*a*	94(3)/6(3)	1/8	1/8	1/8	86(4)
Pt	16*d*	100	1/2	1/2	1/2	53(2)
$Eu_{0.85(2)}Pt_2In_{0.15(2)}$ ($Fd\bar{3}m$)						
Eu/In	8*a*	85(2)/15(2)	1/8	1/8	1/8	84(2)
Pt	16*d*	100	1/2	1/2	1/2	56(2)
$Gd_{0.79(5)}Pt_2In_{0.21(5)}$ ($Fd\bar{3}m$)						
Gd/In	8*a*	79(5)/21(5)	1/8	1/8	1/8	98(4)
Pt	16*d*	100	1/2	1/2	1/2	131(7)
$TmNi_4In$ ($F\bar{4}3m$)						
Tm	4*c*	100	3/4	3/4	3/4	106(2)
Ni	16*e*	100	0.3744(1)	x	x	63(1)
In	4*a*	100	0	0	0	68(2)

All crystallographic data and details for the data collections are listed in Table 2.

The four structures were first refined in the centrosymmetric space group $Fd\bar{3}m$ assuming *RE*/In mixing on the 8*a* site with anisotropic displacement parameters for all atoms using SHELXL-97 (full-matrix least-squares on F^2) [19]. These refinements led to the compositions $Eu_{0.94(3)}Pt_2In_{0.06(3)}$, $Eu_{0.85(2)}Pt_2In_{0.15(2)}$, $Gd_{0.79(5)}Pt_2In_{0.21(5)}$, and $Tm_{0.5}Ni_2In_{0.5}$. The latter composition was indicative of Tm/In ordering. We then refined the structure again in space group $F\bar{4}3m$. Separate refinement of the thulium and indium occupancy parameters confirmed the ordering. Both sites were fully occupied within one standard deviation. Refinement of the Flack parameter [20, 21] indicated twinning by inversion. In the final cycles the batch scale factor (Table 2) was refined as a least-squares variable. Final difference Fourier synthesis revealed no significant residual peaks for all four data sets. The atomic parameters and the interatomic distances are listed in Tables 3 and 4. Further details on the structure refinements are available.*

*Details may be obtained from: Fachinformationszentrum Karlsruhe, D-76344 Eggenstein-Leopoldshafen (Germany), by quoting the Registry No's. CSD 415027 ($Eu_{0.94}Pt_2In_{0.06}$), CSD 415028

Table 4. Interatomic distances (pm), calculated with the lattice parameters taken from X-ray single crystal data of $Eu_{0.94(3)}Pt_2In_{0.06(3)}$, $Eu_{0.85(2)}Pt_2In_{0.15(2)}$, and $Gd_{0.79(5)}Pt_2In_{0.21(5)}$. The distances for $TmNi_4In$ have been calculated with the powder lattice parameters. Standard deviations are all equal or less than 0.1 pm. All distances within the first coordination spheres are listed.

$Eu_{0.94(3)}Pt_2In_{0.06(3)}$				**$Eu_{0.85(2)}Pt_2In_{0.15(2)}$**				**$Gd_{0.79(5)}Pt_2In_{0.21(5)}$**				**$TmNi_4In$**			
Eu/In:	12	Pt	319.5	Eu/In:	12	Pt	318.9	Gd/In:	12	Pt	315.1	Tm:	12	Ni	290.1
	4	Eu/In	333.7		4	Eu/In	333.1		4	Gd/In	329.1		4	In	302.9
Pt:	6	Pt	272.5	Pt:	6	Pt	271.9	Pt:	6	Pt	268.7	Ni:	3	Ni	246.0
	6	Eu/In	319.5		6	Eu/In	318.9		6	Gd/In	315.1		3	Ni	248.5
													3	In	289.8
													3	Tm	290.1
												In:	12	Ni	289.8
													4	Tm	302.9

The crystals investigated on the diffractometers were analyzed in a scanning electron microscope (LEICA 420i) through energy dispersive analyses of X-rays. EuF_3, GdF_3, TmF_3, nickel and platinum metal, and InAs were used as standards. No impurity elements heavier than sodium were observed. The experimentally determined compositions were close to those determined from the structure refinements. Especially the small indium content in $Eu_{0.94}Pt_2In_{0.06}$ was clearly detected *via* EDX.

Results and Discussion

The solid solutions $Eu_{1-x}Pt_2In_x$, $Gd_{1-x}Pt_2In_x$, and $Tm_{1-x}Ni_2In_x$ were investigated on the basis of X-ray powder and single crystal data. In Fig. 2 we present a plot of the unit cell parameters as a function of the compositions. The *a* parameters decrease with increasing indium content. This is due to the substitution of the large rare earth metal atoms (metallic radii of 204, 180, and 175 pm for Eu, Gd, and Tm, respectively) by the smaller indium atoms (163 pm) [22].

The substitution of Eu or Gd by In on the 8*a* site was evident from three single crystals of the solid solutions $Eu_{1-x}Pt_2In_x$ and $Gd_{1-x}Pt_2In_x$. The indium substitution on the rare earth positions is 6 and 15% for the europium and 21% for the gadolinium compound. The lattice parameters show an almost linear decrease from $EuPt_2$ ($GdPt_2$) to $EuPt_4In$ ($GdPt_4In$).

The platinum atoms in $Eu_{0.94}Pt_2In_{0.06}$, $Eu_{0.85}Pt_2In_{0.15}$, and $Gd_{0.79}Pt_2In_{0.21}$ build up a three-dimensional network of corner-sharing $Pt_{4/2}$ tetrahedra (Fig. 1) with Pt–Pt distances of 273, 272, and 269 pm, close to the Pt–Pt distance of 277 pm in elemental Pt [23].

Five samples were investigated by X-ray powder diffraction in the region between binary $TmNi_2$ and ternary $TmNi_4In$. The *a* lattice parameter decreases nearly linearly all the way to $TmNi_4In$ (Fig. 2). The lattice parameters of the sample with the starting composition $Tm_{0.6}Ni_2In_{0.4}$ does not perfectly fit the smooth curve. This is obviously due to a small deviation in the sample composition. The structure of the $TmNi_4In$ single crystal was refined in space group $F\bar{4}3m$ ($MgCu_4Sn$ type structure) and no Tm/In mixing was observed.

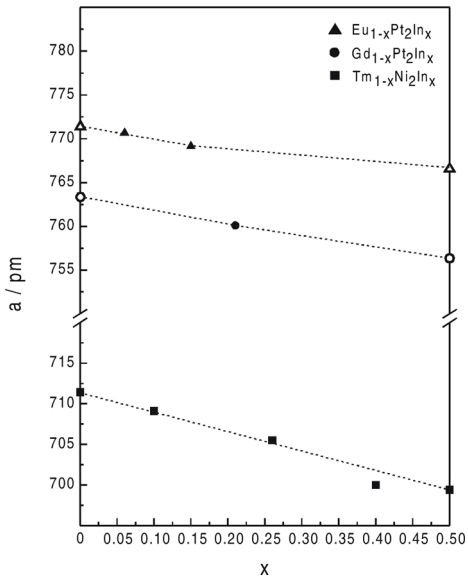

Fig. 2. Course of the unit cell parameters for the solid solutions $Eu_{1-x}Pt_2In_x$, $Gd_{1-x}Pt_2In_x$ and $Tm_{1-x}Ni_2In_x$. The lattice parameters for $Eu_{1-x}Pt_2In_x$ were taken from the single crystal data. The open symbols show the literature data (see Table 1).

Due to the symmetry reduction, the nickel sites in $TmNi_4In$ gain a free structural parameter. Consequently the tetrahedra become slightly distorted with Ni–Ni distances of 246 and 249 pm. The latter com-

($Eu_{0.85}Pt_2In_{0.15}$), CSD 415029 ($Gd_{0.79}Pt_2In_{0.21}$), and CSD 415030 ($TmNi_4In$).

pare well with the average Ni–Ni distance of 249 pm in *fcc* nickel [23].

Both europium containing crystals have been selected from the same sample with the starting composition 0.75 Eu : 2 Pt : 0.25 In. The refined compositions $Eu_{0.94}Pt_2In_{0.06}$ and $Eu_{0.85}Pt_2In_{0.15}$ indicate an inhomogeneity within that sample. In previous studies on the phases $YbNi_{1-x}Sb$ [24] and $La_{2+x}Ge_2Mg_{1-x}$ [25], the inhomogeneities resulted in shoulders for some reflections. As an example we have therefore carefully investigated the 0.75 Gd : 2 Pt : 0.25 In sample with longer counting times on the powder diffractometer. We could only observe small line broadening. The lattice parameters of the different cubic phases $RE_{1-x}Pt_2In_x$ in our samples are too close.

Acknowledgements

We thank Dipl.-Ing. U. Ch. Rodewald and B. Heying for the intensity data collections and H.-J. Göcke for the work at the scanning electron microscope. This work was supported by the Deutsche Forschungsgemeinschaft and the Degussa-Hüls AG. M. L. is indebted to the NRW Graduate School of Chemistry for a PhD stipend.

[1] U. Müller, Anorganische Strukturchemie, Teubner, Stuttgart (1996); Inorganic Structural Chemistry, J. Wiley, Chichester – New York (1993).
[2] P. Villars, L. D. Calvert, Pearson's Handbook of Crystallographic Data for Intermetallic Phases, Second Edition, American Society for Metals, Materials Park, OH 44073 (1991), and desk edition (1997).
[3] A. Iandelli, A. Palenzona, J. Less-Common Met. **80**, P71 (1981).
[4] E. I. Gladyshevskii, P. I. Kripiakevich, M. J. Tesliuk, Dokl. AN SSSR **85**, 81 (1952).
[5] K. Osamura, Y. Murakami, J. Less-Common Met. **60**, 311 (1978).
[6] I. R. Harris, J. Less-Common Met. **14**, 459 (1968).
[7] I. R. Harris, W. E. Gardner, R. H. Taylor, J. Less-Common Met. **31**, 151 (1973).
[8] R. H. Taylor, I. R. Harris, W. E. Gardner, J. Phys. F: Metal Phys. **6**, 1125 (1976).
[9] H. De Graaf, R. C. Thiel, K. H. J. Buschow, Physica B **100**, 81 (1980).
[10] P. I. Kripyakevich, M. Yu. Teslyuk, D. P. Frankevich, Sov. Phys. Crystallogr. **10**, 344 (1965).
[11] R. C. Mansey, G. V. Raynor, I. R. Harris, J. Less-Common Met. **14**, 329 (1968).
[12] E. Burzo, J. Laforest, Int. J. Magn. **3**, 171 (1972).
[13] A. F. Deutz, R. B. Helmholdt, A. C. Moleman, D. B. De Mooij, K. H. J. Buschow, J. Less-Common Met. **153**, 259 (1983).
[14] V. I. Zaremba, V. M. Baranyak, Ya. M. Kalychak, Visnyk Lviv University Chem. Series **25**, 18 (1984).
[15] S. K. Malik, R. Vijayaraghavan, D. T. Adroja, B. D. Padalia, A. S. Edelstein, J. Magn. Magn. Mater. **92**, 80 (1990).
[16] R. Pöttgen, Th. Gulden, A. Simon, GIT-Laborfachzeitschrift **43**, 133 (1999).
[17] R. Pöttgen, A. Lang, R.-D. Hoffmann, B. Künnen, G. Kotzyba, R. Müllmann, B. D. Mosel, C. Rosenhahn, Z. Kristallogr. **214**, 143 (1999).
[18] K. Yvon, W. Jeitschko, E. Parthé, J. Appl. Crystallogr. **10**, 73 (1977).
[19] G. M. Sheldrick, SHELXL-97, Program for Crystal Structure Refinement, University of Göttingen, Germany (1997).
[20] H. D. Flack, G. Bernadinelli, Acta Crystallogr. **55A**, 908 (1999).
[21] H. D. Flack, G. Bernadinelli, J. Appl. Crystallogr. **33**, 1143 (2000).
[22] J. Emsley, The Elements, Oxford University Press, Oxford (1999).
[23] J. Donohue, The Structures of the Elements, Wiley, New York (1974).
[24] R. Mishra, R. Pöttgen, R.-D. Hoffmann, Th. Fickenscher, M. Eschen, H. Trill, B. D. Mosel, Z. Naturforsch. **57b**, 1215 (2002).
[25] R. Kraft, R. Pöttgen, Monatsh. Chem. **135**, 1327 (2004).